

## LATTICE DESIGN FOR PEP-X ULTIMATE STORAGE RING LIGHT SOURCE\*

Yuri Nosochkov, Karl Bane, Yunhai Cai, Robert Hettel, Min-Huey Wang  
SLAC National Accelerator Laboratory, Menlo Park, CA 94025, USA

### Abstract

SLAC expertise in designing and operating high current storage rings and the availability of the 2.2-km PEP-II tunnel present an opportunity for building a next generation light source – PEP-X – that would replace the SPEAR3 storage ring in the future. The PEP-X “baseline” design, with 164 pm-rad emittance at 4.5 GeV beam energy and a current of 1.5 A, was completed in 2010. As a next step, a so-called “ultimate” PEP-X lattice, reducing the emittance to 11 pm-rad at zero current, has been designed. This emittance approaches the diffraction limited photon emittance for multi-keV photons, providing near maximum photon brightness and high coherence. It is achieved by using 7-bend achromat cells in the ring arcs and a 90-m damping wiggler in one of the 6 long straight sections. Details of the lattice design, dynamic aperture, and calculations of the intra-beam scattering effect and Touschek lifetime at a nominal 0.2 A current are presented.

*Presented at the 2<sup>nd</sup> International Particle Accelerator Conference (IPAC 2011)  
San Sebastian, Spain, September 4 – 9, 2011*

---

\* Work supported by the Department of Energy contract DE-AC02-76SF00515.

# LATTICE DESIGN FOR PEP-X ULTIMATE STORAGE RING LIGHT SOURCE\*

Y. Nosochkov<sup>†</sup>, K.L.F. Bane, Y. Cai, R. Hettel, M.-H. Wang  
SLAC National Accelerator Laboratory, Menlo Park, CA 94025, USA

## Abstract

SLAC expertise in designing and operating high current storage rings and the availability of the 2.2-km PEP-II tunnel present an opportunity for building a next generation light source – PEP-X – that would replace the SPEAR3 storage ring in the future. The PEP-X “baseline” design, with 164 pm-rad emittance at 4.5 GeV beam energy and a current of 1.5 A, was completed in 2010. As a next step, a so-called “ultimate” PEP-X lattice, reducing the emittance to 11 pm-rad at zero current, has been designed. This emittance approaches the diffraction limited photon emittance for multi-keV photons, providing near maximum photon brightness and high coherence. It is achieved by using 7-bend achromat cells in the ring arcs and a 90-m damping wiggler in one of the 6 long straight sections. Details of the lattice design, dynamic aperture, and calculations of the intra-beam scattering effect and Touschek lifetime at a nominal 0.2 A current are presented.

## INTRODUCTION

Accelerator-based light sources are in high demand for many experimental applications. The availability of the 2.2-km PEP-II tunnel at SLAC presents an opportunity for building a next generation light source - PEP-X – that would replace the existing SPEAR3 light source in the future. The PEP-X study started in 2008, and the “baseline” design, yielding 164 pm-rad emittance at 4.5 GeV beam energy and a current of 1.5 A, was completed in 2010 [1]. This relatively conservative design can be built using existing technology.

However, for a long term future, it is natural to investigate a more aggressive, so-called “ultimate” ring design [2]. The goal is to reduce the electron emittance in both  $x$  and  $y$  planes to near the diffraction limited photon emittance of 8 pm-rad at hard X-ray photon wavelength of 0.1 nm. This would provide a near maximum photon brightness and significant increase in photon coherence.

This study was motivated by the advances in low emittance design at MAX-IV [3]. The latter was used as a starting point for the PEP-X arc lattice, however new features were included into the design for better tuning capabilities and compensation of non-linear optics effects. Further emittance reduction is achieved with a 90-m damping wiggler. Finally, intra-beam scattering (IBS) and Touschek lifetime effects were estimated and cross-checked using various codes.

## LATTICE

In order to fit into the 2.2 km PEP-II tunnel, the PEP-X ring adopts the PEP-II geometry as shown in Fig. 1, where the arcs and long straight sections are labeled from 1 to 12.

### Arc Cell

An ultimate ring lattice must push emittance to the new low levels while providing dispersion-free optics for insertion devices (IDs) and sufficient dynamic aperture for injection and beam lifetime. For a given beam energy, emittance  $\epsilon_0$  is a function of cell optics, dipole bending angle  $\theta$  and horizontal damping partition number  $J_x$ :  $\epsilon_0 \propto F \theta^3 / J_x$ . Theoretical Minimum Emittance (TME) cells have the lowest optics factor  $F$ , but lack dispersion-free straight. On the other hand, Double Bend Achromat (DBA) cells, often used in light source rings, provide ID straights, but have a factor of 3 higher emittance. The solution is a hybrid cell – a multi-bend achromat – comprised of TME units and a dispersion matching unit (as in half DBA) at each end.

The desired small bending angle per dipole implies a large number of very compact TME units per arc. An example is the MAX-IV 7-bend achromat cell [3], where TME defocusing quadrupoles are eliminated and replaced by defocusing gradients in dipoles, and sextupole magnets are integrated with dipoles or quadrupoles in compact blocks. A defocusing gradient in the dipole has the added advantage of higher  $J_x$  for even lower emittance.

The PEP-X arc cell, shown in Fig. 2, is similar to the MAX-IV design with a few modifications. It has a natural emittance of 29.0 pm-rad at 4.5 GeV and zero current. The cell phase advance  $\mu_x / \mu_y = 2\frac{1}{8} / 1\frac{1}{8} [\times 2\pi]$  provides optimal non-linear lattice properties discussed later. The cell length is 30.4 m, yielding 8 cells per arc. The TME units are made of focusing quadrupoles and dipoles with defocusing gradient, and have periodic lattice functions. A matching dipole at each cell end is gradient-free and 20% shorter than the TME dipole. The 5.0-m ID straight

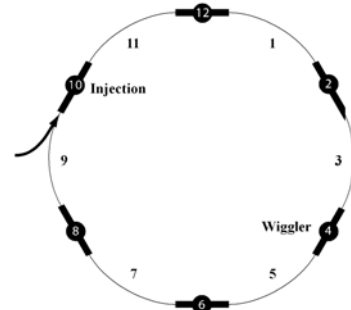


Figure 1: PEP-X layout with 6 arcs and 6 long straights.

\* Work supported by the Department of Energy Contract DE-AC02-76SF00515.

<sup>†</sup> yuri@slac.stanford.edu

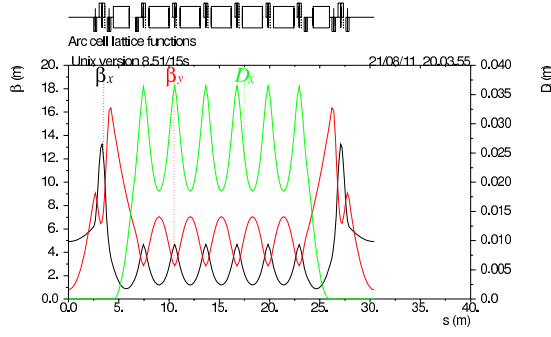


Figure 2: Lattice functions in PEP-X 7-bend achromat cell.

has  $\beta_x/\beta_y = 4.9/0.8$  m at the ID center. The ID  $\beta_y$  is near its optimal value of  $L_{ID}/2\pi$  for maximum brightness. Compared to MAX-IV, this cell has 4 additional matching quadrupoles to provide a larger tuning range of the ID  $\beta$  functions. As shown in Fig. 3, the ID  $\beta_y$  can be changed to up to 5 m value while the cell phase advance is fixed and the ID  $\beta_x$  and cell emittance are not significantly changed.

At present, a thin lens sextupole model is used. Four families of chromaticity correcting sextupoles are placed at center of quadrupoles and at each end of dipole where dispersion is not zero. Additionally, 6 harmonic sextupoles are placed in the dispersion-free quadrupole triplets adjacent to the ID straights. This scheme provides sufficient flexibility for optimization of non-linear momentum and amplitude dependent optics perturbations discussed further in [4].

### Non-linear Properties

One of the challenges of a low emittance lattice is maintaining a sufficient dynamic aperture for injection and beam lifetime. Shorter cells lead to stronger quadrupoles and higher ring chromaticity, while weaker dipoles reduce dispersion resulting in stronger chromatic correction sextupoles. The latter produce a larger non-linear field on a particle trajectory leading to a smaller dynamic aperture.

To keep dynamic aperture large, the non-linear sextupole effects must be minimized. To do so, we apply the K. Brown's theorem stating that a system of  $\geq 4$  identical cells with a total linear matrix of +I in both planes cancels 2nd order matrix geometric terms [5]. This is equivalent to cancellation of the sextupole 3rd order geometric resonance driving terms. The PEP-X cell phase advance  $\mu_x/\mu_y = 2\frac{1}{8}/1\frac{1}{8}[\times 2\pi]$  is chosen to attain a +I matrix per

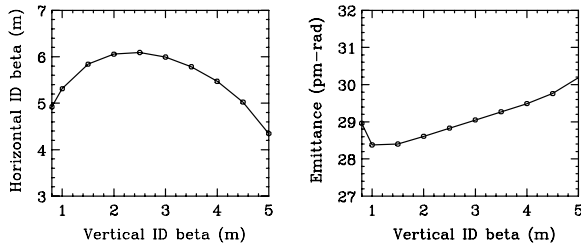


Figure 3: Variation of  $\beta_y$  function at ID center and its effect on ID  $\beta_x$  (left) and natural cell emittance at 4.5 GeV (right).

each arc of 8 cells and provide an optimal linear optics. This cancels all sextupole 3rd order geometric resonance driving terms within each arc, confirmed by the LEGO [6] calculation in Fig. 4 using differential algebra and Lie formalism [7]. The choice of 8 cells per arc also results in similar cancellation of the 2nd order dispersion and all sextupole 4th order geometric resonance driving terms, except  $2\nu_x - 2\nu_y$ , as shown in Fig. 5. Such compensation works for any cell sextupole scheme as long as the cells are identical. However, amplitude dependent tune shifts are not canceled and were reduced through sextupole optimization [4].

In a similar way, a high ring periodicity helps to suppress some of the systematic resonances. While PEP-X has 6 identical arcs and 5 identical long FODO straights, the injection straight-10 in Fig. 1 has a special optics. In general, this non-periodicity reduces dynamic aperture as compared to a 6-fold ring. Nonetheless, a solution was found to restore the effective 6-fold periodicity by making the injection straight linear matrix the same as in other straights. This required that fractional part of phase advance in all straights is the same. This adjustment restored the dynamic aperture to the level of an ideal 6-fold ring aperture.

### Damping Wiggler

With the 29 pm-rad natural emittance of the arcs, a damping wiggler in a dispersion-free region is necessary in order to reduce the emittance another factor of 3 for approaching the 0.1-nm X-ray diffraction-limited emittance. A relative emittance reduction from the wiggler can be analyzed using theoretical expressions such as in [8]. In general, it depends on wiggler period length, wiggler peak

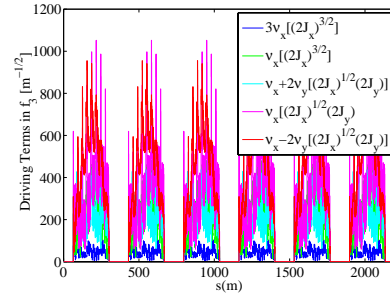


Figure 4: Accumulation and cancellation of sextupole 3rd order resonance driving terms within each arc.

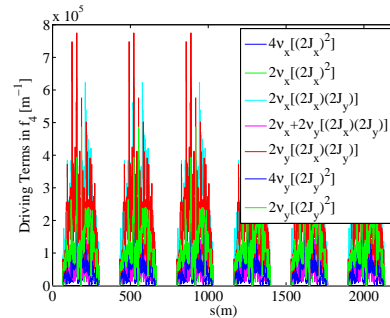


Figure 5: Accumulation and cancellation of sextupole 4th order resonance driving terms within each arc.

field, and the total wiggler length. The analytical dependence on the wiggler field and length for various values of wiggler period is shown in Fig. 6 where the wiggler is inserted in the long straight section with  $\langle \beta_x \rangle = 12.4$  m. One can see that most of the damping occurs within 100 m of wiggler length. It is also evident that wiggler period below 5-cm does not significantly improve the damping. Assuming a 90-m wiggler with 5-cm period, it follows that the optimal peak field is 1.5 T. Note that a shorter period requires a smaller wiggler gap when using a hybrid magnet design [1]. Modeling of a realistic wiggler magnet is in progress. In the present lattice, the wiggler is approximated using a sequence of alternating field 2.5-cm dipoles separated by 2.5-cm gaps. It is placed in the straight-4 in Fig. 1, where it is split into 18 sections to fit between the quadrupoles. The resultant PEP-X emittance at zero current is  $\epsilon_0 = 11$  pm-rad. One negative wiggler effect is an increase of rms energy spread from 0.072% to 0.12%.

The optimized PEP-X dynamic aperture at the injection point where  $\beta_x = 200$  m, without errors and with the above wiggler model, is shown in Fig. 7 for  $\Delta p/p$  from 0 to 2%. Based on the baseline study [1], this is sufficient for off-axis injection assuming high quality injected beam with 1  $\mu$ m-rad normalized emittance and effective septum width of 3 mm. It is noted that on-axis injection could be used to accommodate a lattice with smaller dynamic aperture.

## IBS AND TOUSCHEK LIFETIME

IBS and Touschek effects, which increase emittance and cause particle loss through change of particle momentum, tend to be important in low emittance machines. To maintain both  $x$  and  $y$  emittances near the level of the diffraction-limited photon emittance, we consider a fully coupled PEP-X beam with emittance of  $\epsilon_{x0} = \epsilon_{y0} = \epsilon_0/2 =$

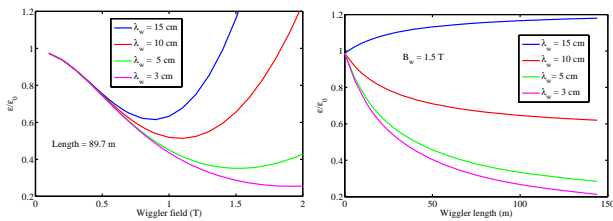


Figure 6: Emittance reduction versus wiggler field (left) and length (right) for various values of wiggler period.

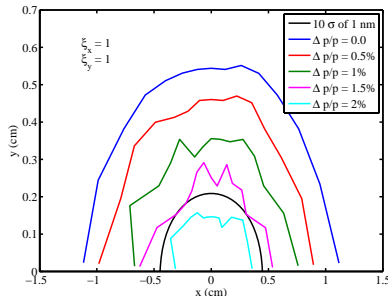


Figure 7: PEP-X dynamic aperture without errors.

5.5 pm-rad at zero current. We further assume that vertical dispersion is negligible. Solving the Bjorken-Mtingwa (BM) equations [9] for IBS growth rates but treating  $x$ - $y$  coupling in a simple manner, we find that, at the PEP-X nominal beam current of 0.2 A, the steady-state emittances are  $\epsilon_x = \epsilon_y = 11.8$  pm, while growth of the rms bunch length and energy spread is small. This result is in a good agreement with simulations using SAD [10], a program that more accurately simulates coupling and can also solve the BM equations.

Touschek lifetime calculations require the knowledge of momentum aperture and normally follow the flat-beam equation of Brück [11]. For a round PEP-X beam, we use the more general formula of Piwinski [8]. The resultant Touschek lifetime is 1.6 hrs determined by an average momentum aperture of  $\pm 1.6\%$  in the PEP-X arcs. The complete list of PEP-X parameters is shown in Table 1.

Table 1: PEP-X parameters at 0.2 A beam current.

Energy [GeV]	4.5
Circumference [m]	2199.3167
Tune, x/y/s	113.23 / 65.14 / 0.0069
Beam current [A]	0.2
Coupling, %	100
Emittance, x/y [pm-rad]	11.8 / 11.8
Bunch length [mm]	3.1
Energy spread	$1.25 \cdot 10^{-3}$
Momentum compaction	$4.96 \cdot 10^{-5}$
Damping time, x/y/s [ms]	19 / 22 / 12
Natural chromaticity, x/y	-162.3 / -130.1
Energy loss per turn [MeV]	2.95
RF voltage [MV]	8.3
RF frequency [MHz]	476
Wiggler length/period [m]	89.66 / 0.05
Wiggler peak field [T]	1.5
Length of ID straight [m]	5.0
Beta at ID center, x/y [m]	4.92 / 0.80
Touschek lifetime [hr]	1.6

## ACKNOWLEDGMENTS

We thank K. Kubo and M. Borland for verifying our IBS calculations with SAD [10] and ELEGANT [12] codes.

## REFERENCES

- [1] K.L.F. Bane *et al.*, SLAC-PUB-13999 (2010).
- [2] M.Bei *et al.*, Nucl. Instr. Meth. **A622**, p. 518 (2010).
- [3] S.C. Leemann *et al.*, Phys. Rev. ST-AB **12**, 120701 (2009).
- [4] M-H. Wang *et al.*, THPC074, this conference.
- [5] K. Brown, IEEE Trans. NS, **NS-26**, No. 3 (1979).
- [6] Y. Cai *et al.*, SLAC-PUB-7642 (1997).
- [7] Y. Cai, Nucl. Instr. Meth. **A645**, p. 168 (2011).
- [8] “Handbook of Accelerator Physics and Engineering”, edited by A. Chao and M. Tigner, World Scientific (2006).
- [9] J.D. Bjorken, S.K. Mtingwa, Part. Accel. **13**, 115 (1983).
- [10] <http://acc-physics.kek.jp/SAD/>.
- [11] H. Brück, Accélérateurs Circulaires de Particules (1966).
- [12] M. Borland, APS Tech. Rep. LS-287 (2000).